First-principles investigation of the structural and electronic properties of self-assemblies of functional molecules on graphene

Ambroise J Quesne-Turin, Jeremy J Touzeau, Yannick J Dappe, Boubakar Diawara, François J Maurel, Mahamadou J Seydou

Superlattices and Microstructures 105 (2017) 139–151

Contents lists available at ScienceDirect

Superlattices and Microstructures

journal homepage: www.elsevier.com/locate/superlattices

First-principles investigation of the structural and electronic properties of self-assemblies of functional molecules on graphene

Ambroise Quesne-Turin [a], Jeremy Touzeau [a], Yannick J. Dappe [b], Boubakar Diawara [c], François Maurel [a], Mahamadou Seydou [a, *]

[a] Université Paris Diderot, Sorbonne Paris Cité, ITODYS, UMR 7086 CNRS, 15 Rue J.-A.de Baïf, 75205 Paris Cedex 13, France
[b] SPEC, CEA, CNRS, Université Paris-Saclay, CEA Saclay, 91191 Gif-sur-Yvette Cedex, France
[c] Département Moissan, FR 3203, CNRS-ENSCP, Ecole Nationale Supérieure de Chimie de Paris, 11 Rue Pierre et Marie Curie, 75005 Paris, France

ARTICLE INFO

Article history:
Received 22 December 2016
Received in revised form 18 March 2017
Accepted 19 March 2017
Available online 20 March 2017

Keywords:
Self-assembly
Graphene
Supramolecular network
DFT
Adsorption
Hydrogen bonds
DOS

ABSTRACT

Graphene-based two-dimensional materials have attracted an increasing attention these last years. Among them, the system formed by molecular adsorption on, aim of modifying the conductivity of graphene and make it semiconducting, is of particular interest. We use here hierarchical first-principles simulations to investigate the energetic and electronic properties of an electron-donor, melamine, and an acceptor, NaphtaleneTetraCarboxylic DiImide (NTCDI), and the assembly of their complexes on graphene surface. In particular, the van der Waals-corrected density functional theory (DFT) method is used to compute the interaction and adsorption energies during assembly. The effect of dispersion interactions on both geometries and energies is investigated. Depending on the surface coverage and the molecular organization, there is a significant local deformation of the graphene surface. Self-assembly is driven by the competition between hydrogen bonds in the building blocks and their adsorption on the surface. The dispersion contribution accounts significantly in both intermolecular and adsorption energies. The electron transfer mechanism and density of states (DOS) calculations show the electron-donor and acceptor characters of melamine and NTCDI, respectively. Molecular adsorption affects differently the energy levels around the Fermi level differently, leading to band gap opening. These results provide information about the new materials obtained by controlling molecular assembly on graphene.

1. Introduction

In order to develop materials and devices with innovative properties, controlling the structure and organization of molecules at the nanoscale on a surface is a subject of great interest in nanosciences [1–3].

In addition to making it possible to reduce device size, molecular or metallic nanostructures exhibit original size-dependent properties in such diverse fields as optics, magnetism, electrochemistry, molecular and organic electronics

* Corresponding author.
E-mail address: mahamadou.seydou@univ-paris-diderot.fr (M. Seydou).

http://dx.doi.org/10.1016/j.spmi.2017.03.034
0749-6036/

[4–8]. However, the control of these properties is related to the ability to adapt the spatial organization and arrangement of these nanostructures.

One route developed in the recent years to build nano-structured surfaces is based on supramolecular chemistry [9]. This route allows one to create specific architectures through self-assembly of specific functional building blocks which are controlled by various types of interactions (electrostatic, hydrogen bonding, van der Waals, coordination chemistry …).

An appropriate choice of building blocks gives access to a wide range of nano porous architectures. The size of the organized pores ranges from 0.5 to a few nanometers. It has been shown that molecular networks on surface can be considered as host systems with proven ability to accommodate guests of different natures, as well as an important control of the guest domains dimensions. In this respect, melamine and its derivatives are the most common building blocks used to form molecular two-dimensional molecular networks on metal surfaces [10–16]. Indeed, their hydrogen-bond receptor and acceptor moieties of hydrogen bonds allow them to self-assemble easily either alone or combined with other donors or acceptors.

Among the different intermolecular forces determining molecular self-assembling on surfaces, hydrogen bonding is particularly interesting as a driving force to develop supramolecular networks. Indeed, it is directional and settles spontaneously, provided that the interacting molecules have donor and acceptor sites for hydrogen bonds. However, from a theoretical point of view, the nature of intermolecular forces (non-local, weak and long range) makes them complicated to model them accurately at the atomic scale. In particular, Density Functional Theory (DFT), which has become a common technique for describing electronic systems at the atomic level, fails to describe interactions like hydrogen bonds or molecular adsorption on surface through van der Waals interactions (vdW) [17]. Fortunately, improvements have been made in the recent years to provide a better description of those interactions in the framework of DFT [12,18].

In practice, most of the molecular self-assembling studies are carried out on metallic surfaces, under vacuum or at solid-liquid interface, using for example the high symmetric functional melamine [13–15], NaphtaleneTetraCarboxylic Dilmide (NTCDI) [18–21], and derived molecules [15,22–24]. This has led to adjust the procedures of development of various self-assembled patterns on Au (111), Ag(111), Cu(111) or Si(111) surfaces.

The last decade, graphene as an ideal surface for molecular self-assembly [25] has attracted the attention of scientists in the field because of its large planar surface area, its ability to form strong π-stacking interactions with planar conjugated molecules and the exceptional growth of its based two-dimensional materials [26–30].

For example, it was shown that melamine and cyanuric acid can self-organize on graphite surface [31] through hydrogen bonding, and form a hexagonal pore network similar to those observed on a gold surface [13]. More recently, the adsorption of melamine on graphene was studied, combined plasma exposure, Raman spectroscopy and DFT calculations showing that the charge density can be tuned by adsorption of melamine on graphene surface defects [32]. The self-assembly of perylene derivative [33,34] biological molecules [35], porphyrin or phthalocyanin compounds [36,37] and other polycyclic molecules [38–40] on graphene sheet has also been performed, demonstrating a well organized two dimensional networks. At the fundamental level, to understand graphene and molecular interactions better, the adsorption of small molecules [41,42] as well as heavy metallic atoms [43]was investigated; this reveals the different chemical and physical processes that can occur.

In this context, the present work aims at theoretically investigating melamine, NTCDI and their complex adsorption process at low and high coverage. For the latter, graphene sheet nanostructuration has been considered through the self-assembly of NTCDI and melamine molecules. The establishment of hydrogen bonds between the amine and carboxylic groups allows the formation of a two-dimensional pore network.

The formation of this two dimensional network has been studied in absence or presence of the surface in order to analyze the competition between the intermolecular interactions and adsorption energies on graphene monolayer. Using DFT combined with an empirical model taking into account vdW interactions [44], we have tested the influence of dispersion interactions on the molecular self-assembly on graphene. The surface coverage rate is varied by increasing from one molecule on a large super cell to the formation of a molecular network (with a high density of molecules). The electronic properties such as density of states (DOS) and band structures have been computed and compared to literature and previous experimental results. The effect of molecular adsorption on the graphene band structure is of particular interest since it was shown that it can lead to a band gap opening [33,38]. In the present work, we obtain 100 meV bandgap opening, paving the way to semiconducting behavior of graphene. Moreover, the mechanical properties of deformed graphene can lead to potential applications in tunable nanoelectronics.

2. Calculation method

Calculations were performed using Density Functional Theory (DFT) as implemented in the Vienna Ab Initio Simulation Package (VASP 5.2.11) [45,46]. Electron-ion interactions were described by the projector-augmented wave (PAW) [47,48] method. Convergence of the plane-wave expansion was obtained using a cut-off of 500 eV. The generalized gradient approximation (GGA) was used with the Perdew-Burke-Ernzerhof functional (PBE) [49,50]. Sampling in Brillouin zone was performed on a grid of $5 \times 5 \times 1$ k-points for the geometry optimizations and $15 \times 15 \times 1$ for density of states (DOS) calculations. The ionic positions are fully-optimized with Hellman-Feynman tolerance of 0.01 eV/Å. The energy tolerance of the electronic minimization is 10^{-6} eV. All the computations reported in this paper were performed using the dispersion-including DFT Grimme D2 method [51]. This method describes the dispersion interactions between a particle and its neighbors in a given radius, via a simple pair-wise force field summed with the pure DFT energy:

$$E = E_{DFT} + E_{D2} \tag{1}$$

The procedure for building of the two-dimensional molecular networks is the one established by Kantorovitch et al. [13] and used for NTCDI self-assembly [19]. Melamine and NTCDI monomers are built and fully optimized, and then used to build the corresponding dimers. Starting from the different dimer molecular complexes in the gas phase, the most stable 2D supramolecular networks were built by translation of repeating units in the two-dimensional space.

The stabilization energy in vacuum ΔE^{V}_{stab} is calculated using formula (2).

$$\Delta E^{V}_{stab} = \frac{E(M_n) - n \times E(M)}{n} \tag{2}$$

where $E(M_n)$ is the energy of the complex (dimer) or monolayer in a unit cell, in absence of the surface, E(M) is the energy of the optimized monomer and n the total number of molecules in the unit cell.

As the intermolecular interactions originate essentially from hydrogen bonds, the average interaction per hydrogen bond (ΔE_{LH}) is evaluated as the ratio between total stabilization energy and the total number of hydrogen bonds m formed in the complex.

$$\Delta E_{LH} = \Delta E^{V}_{stab} / m \tag{3}$$

The most stable topologies were retained for their use in the study of their interaction with the carbon surface, and the adsorption energies (ΔE_{ads}) are calculated as follows:

$$\Delta E_{ads} = \frac{\left[E(M_{n,ads}) - nE(M) - E(G)\right]}{n} \tag{4}$$

where $E(M)$ and $E(G)$ are the total electronic energies of Molecule and graphene surface, respectively, obtained after separate geometry optimization. $E(M_{n,\ ads})$ is the energy of the optimized (n.Molecule-assembly + Graphene surface system), n being the number of molecules per unit cell. To better understand the adsorption process, the melamine, NTCDI and their complexes (see Fig. 1) were assembled in vacuum and on the graphene surface. The total stabilization energy of the adsorbed network on graphene is evaluated as the sum of adsorption energy and the hydrogen bonds contribution.

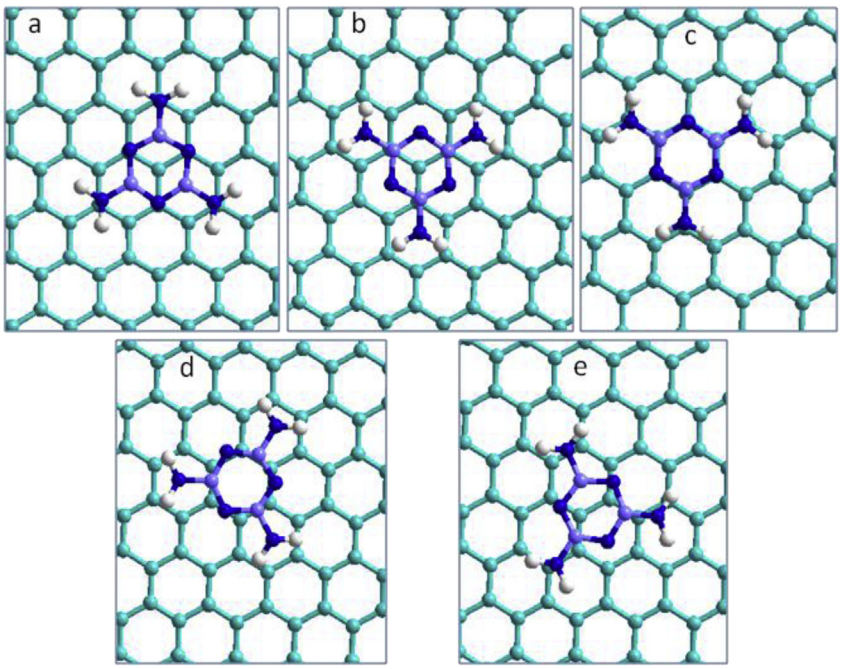

Fig. 1. Optimized structures of melamine on different adsorption sites upon graphene: topC-top (a), N-top (b), All-top(c), cross (d), bridge (e). Graphene carbon atoms are in cyan, nitrogen in blue, hydrogen in white, carbon of melamine in lilas. (For interpretation of the references to colour in this figure legend, the reader is referred to the web version of this article.)

$$\Delta E^{S}_{stab} = \Delta E_{ads} + \Delta E^{V}_{stab} \quad (5)$$

3. Results and discussion

Melamine $C_3N_6H_6$ (See Scheme 1) has three amine groups (of hydrogen donor), allowing hydrogen bonding with the nitrogen atoms of the central ring (hydrogen acceptor) of another molecule. The optimized structure of the melamine is flat, apart from the hydrogens of the amino groups which tend to move slightly out of the plane of the ring due to the sp^3 hybridization character of the nitrogen atom which bears them.

We use the same methodology as references to build gradually the assembly of melamine [13,18], NTCDI [19] and their complexes in the absence of surface.

3.1. Melamine assembly on surface

The geometries of molecules and networks, previously optimized (See Supplementary document Fig. S1 and Table S1) are deposited on the graphene surface. The main purpose here is to evaluate the role of the surface in the assembly at each step from monomer to 2D network.

Monomers and dimers were placed on a large cell so to be isolated from their neighboring cells images. This corresponds to a (8×8) graphene supercell of 128 carbon atoms. For the networks, the supercell whose bases vectors are closest to the molecular network is built and optimized. Note that sometimes, commensurability problems arise and the molecular network is slightly deformed to adapt the network to the surface. When the deformation is significant, the calculations present errors that can compromise the comparison of the systems.

The calculation procedure is the following: we have positioned the adsorbate at variable distances from the graphene surface and calculated single point energy of the system as a function of this distance. This gave us the potential energy curve for the approach of the adsorbate. This potential is attractive up to the equilibrium distance, and becomes repulsive for shorter distances. Doing so, we assume that we start the relaxation with a good initial configuration. All calculations were performed in absence and presence of dispersion interactions in the total energy.

3.1.1. Monomer: rotation and translation configurations

We have explored several adsorption sites of the isolated melamine on the large graphene sheet as shown on Fig. 1. Five configurations corresponding to different adsorption sites are built, depending on the rotation or translation of melamine around its center of mass. For each site, the whole system has been fully optimized and the adsorption energies have been calculated. The optimized geometries of theses configurations so called C-top, N-top, All-top, cross, and bridge are stable and presented on Fig. 1.

For each site, we vary the distance of the melamine molecule to the surface from 4.00 to 2.40 Å. The equilibrium distance varies between 2.60 and 2.80 Å for different sites. From the equilibrium distance, we perform a full relaxation of the geometry of the complexes and calculate the adsorption energies of each site, as reported in Table 2.

The adsorption energies are found to be equal to −0.954, −0.901, −0.165, −0.947 and −0.233 eV for C-top, N-top, All-top, cross and bridge, respectively. Dispersion correction contributes to the standard DFT energy values of −0.434, −0.387, −0.533, −0.298, and −0.647 eV per molecule for C-top, N-top, All-top, cross and bridge, respectively. The most stable configurations correspond to the C-top, N-top and cross for which the carbon or nitrogen atoms take place in the center of graphene rings. These minimum adsorption energy is closed to the value in Ref. [52] and smaller than the value of −1.720 eV found by Medina and coauthors [32] for the melamine adsorption on a (6×6) graphene supercell. The difference originates probably from the basis set superposition error (BSSE) associated with the use of finite localized orbital method by the authors. Using DFT and plane wave method without dispersion correction, Chang and coauthors [53] found the cross configuration as the most stable for triazine molecule with an adsorption energy of −0.344 eV, less than the one found for melamine (−0.954 eV) because of the difference in the number of nitrogen atoms in the two molecules. Using dispersion corrected semi-empirical method

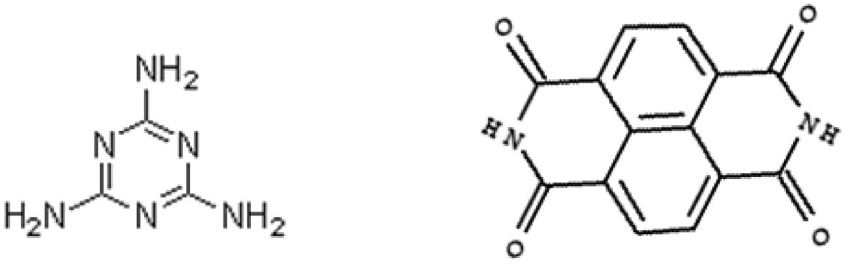

Scheme 1. Chemical structures of melamine (left) and NTCDI (right).

(PM6-DH2), an adsorption energy of −70 and −500 meV per carbon atom was found for aromatic hydrocarbons [54] and carbon nanotube [55], respectively on large graphene sheet in agreement with experimental measurements. Adsorption energy values of −1.358, −1.977 and −1.329 eV are found for 2,3,5,6-tetrafluoro-7,7,8,8-tetracyanoquinodimethane (F4-TCNQ), tetrathiafulvalene (TTF) and the electron acceptor tetracyanoethylene (TCNE), respectively [56].

After optimization, we observed a significant deformation of the graphene layer under the molecule for the most energetically favorable positions. This deformation can reach 1.80, 1.49, and 1.68 Å for C-top, hollow and cross sites (Table 1). Also, a little deformation is found for the less stable structure (bridge). The minimum graphene-melamine distance varies from 2.25 to 2.72 Å for the most stable adsorption sites and increases up to 3.18 Å for the less stable. However, the aromatic ring of melamine is not deformed; meanwhile the hydrogen atoms have different orientations depending on the adsorption site. For the less stable configuration, for which graphene is little deformed, we observed that the hydrogens are oriented towards the graphene surface and the NH_2 seem to keep their sp^3 hybridization. For the most stable configurations, graphene is greatly deformed under the molecule. The hydrogen atoms remain in the same plane as the edge of the valley created. They establish an (NH-π) interaction with the edge of the valley. For these configurations, the nitrogen atoms have a more pronounced sp^2 hybridization character. Melamine being less stable in its planar configuration, the energy of stabilization is more important. Previously, the study of nucleobases adsorption on graphene demonstrates that N–H … π interactions in addition to lone pair-π contacts play a crucial role in stabilizing such kinds of systems [57].

3.1.2. Melamine assembly on the graphene sheet: from dimer to 2D networks

As for the monomer, the melamine dimer is deposited on the surface of the (8 × 8) supercell which is large enough to inhibit the interactions between the molecules and their images. In one dimension, for the three chains A, B, and C, we use graphene supercell (4 × 6), (5 × 6) and (3 × 6) respectively, which fit better with the networks lattice vectors and annihilate the interactions between the chain and its images. We define the missing fit as the difference between the chain lattice vector and the graphene supercell vector used to describe the adsorption of this chain. In this cases, the missing fit with the surface is lower for B (0.8%) chains and rather significant for A (−7.2%) and C (−5.4%). For the 2D networks (4 × 4) and (3 × 5), supercells are used to adsorb the porous and compact hexagonal networks, respectively. They correspond to missing fits of 5.3% and 8.8% for the porous and compact networks, respectively.

The formed complexes are fully relaxed. The calculated adsorption energies per molecule are reported in Table 1 and equal to −0.906, −1.502, −0.293 and −0.571 eV/molecule for the dimer, 1D chains B, 2D-compact and 2D-porous hexagonal networks, respectively. The calculated adsorption energy of the dimer is in a good agreement with reference [52] where it is found equal to −0.967 eV per molecule. While the dimer and monochain adsorptions are clearly exothermic, for the two dimensional network, the adsorption energy increases and becomes less exothermic for the compact and porous networks. The hexagonal porous network adsorption is more favorable than the compact one, in particular when dispersion contributions are considered, probably due to the smaller missing fit.

Contrary to the dimer case, only a small buckling with corrugation of graphene sheet below 0.20 Å is observed (See Fig. 2). Also, the minimum distances between the molecular network and the graphene surface become more important, reaching 2.93, 3.27, 3.28 and 3.47 Å for the dimer, monochain B, compact and porous network, respectively (Table 1). On a geometrical point of view, the compact hexagonal network becomes flat, whereas in the absence of surface, melamine molecules were tilted with respect to the plane of the repeating unit.

The adsorption and self-organization process are characterized by the interplay between molecule-molecule and molecule-surface interactions. The most important is the intermolecular interaction and the less important one is the molecule-surface interaction. Fig. 3 presents the global stabilization energy due to the adsorption and the self-assembly for different sizes. The adsorption energy ΔE_{ads} increases from the monomer to the 2D-network, while the vacuum stabilization energy ΔE^{V}_{stab} decreases.

Table 1
Calculated adsorption energies per molecule without and with inclusion of dispersion contribution and the minimum and maximum vertical spacing for isolated melamine, dimer, 1D chains and 2D-networks adsorption on graphene. (Energies in eV and distances in Å).

Melamine		$\Delta E_{ads\ (PBE)}$		$\Delta E_{ads\ (PBE\text{-}D2)}$	Vertical spacing	
System	Configuration	This work	Ref [52]	This work	Min	Max
monomer	C-top	−0.954	−1.055	−1.388	2.72	4.43
	N-top	−0.901	–	−1.288	2.48	3.95
	All-top	−0.165	–	−0.698	3.22	3.62
	Bridge	−0.233	–	−0.880	3.18	3.67
	Cross	−0.947	–	−1.245	2.71	4.39
dimer		−0.411	−0.967	−0.906	2.93	4.44
1D	A	−0.771	–	−1.312	3.22	3.42
	B	−0.168		−1.502		
	C					
2D	compact	0.204	–	−0.293	3.28	3.43
	hexagonal	−0.108	–	−0.571	3.47	3.48

Table 2
Calculated adsorption energies per molecule without and with inclusion of dispersion and the vertical spacing for the considered NTCDI (and NTCDI-melamine complex) monomer, dimers, and 2D network adsorbed on graphene. (Energies in eV and distances in Å).

NTCDI		ΔE_{ads}		M-G vertical spacing	
System	Conf.	(PBE)	(PBE-D2)	Min	Max
monomer		0.051	−1.191	3.15	3.50
Dimer	D1	−0.551	−1.466	2.21	4.40
	D2	−0.436	−1.553	2.79	4.22
	D3	−0.535	−1.745	2.69	4.36
2D network	R3P	−0.786	−1.901	3.55	3.57
Melamine/NTCDI complex					
Dimer	A	−1.975	−3.450	2.65	4.61
	B	−2.886	−3.582	2.36	4.97
	C	−1.989	−3.501	2.48	4.44
2D-network		−3.125	−6.895	2.13	4.72

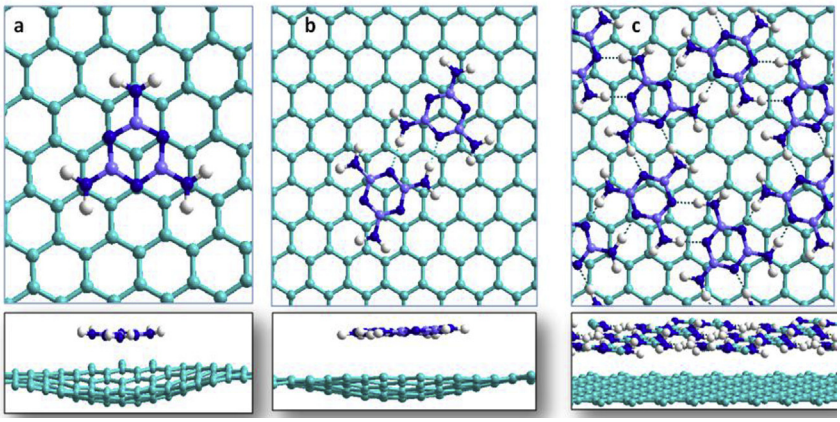

Fig. 2. Optimized structures of melamine (C-top) (a), dimer (b) and porous hexagonal network (c) on graphene. To distinguish the carbon atoms of graphene and the adsorbate, the carbon atoms of the adsorbate are represented in lilas.

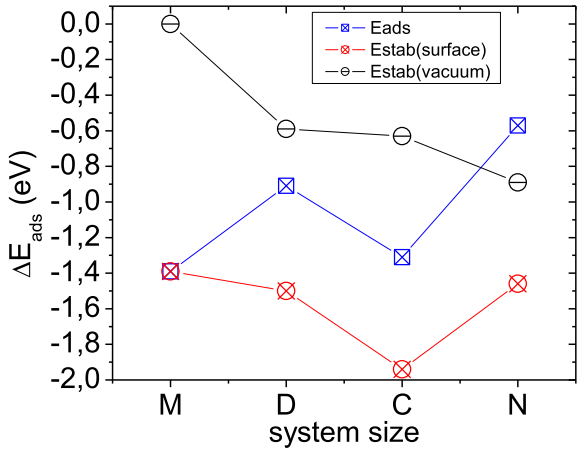

Fig. 3. Stabilization and adsorption energies variation as a function of the melamine cluster size. M, D, C, N stand respectively for Monomer, Dimer, Chain and Network of melamine.

In practice, to form a supramolecular network, the molecules are dispersed in the solvent, and then deposited by drop on the surface on which they self-assemble after evaporation of the solvent. In this training process, the respective roles of the solvent and the surface are not obvious. Theoretical calculations can provide valuable information to assist in the understanding of this process. Considering our thermodynamic results without entropic correction, in absence of solution, the adsorption of single or dimer molecules is clearly favorable, while the network adsorption is endothermic. The calculated

stabilization energy in vacuum and on the surface as well as the adsorption energy are plotted as a function of the size of the molecular organization from monomer to 2D-network on Fig. 3. The results show an increase of adsorption from monomer to network formation, while the total stabilization energy on the surface decreases in the same range. It appears clearly that the presence of the surface enhances the stabilization energy compared to the vacuum. As a consequence, we can suppose that melamine molecules are adsorbed alone or through dimers before forming a supramolecular network. The limits of this affirmation concern the calculations errors, the loss of entropic correction and the kinetic of adsorption and solvation effect. In this context, it was shown recently that enthalpy gain is dominated by solvation and dewetting, which lowers the entropic cost and render monolayer self-assembly a thermodynamically favored process [58].

3.2. Melamine complexation with NTCDI on graphene sheet

NTCDI molecules assembly in absence of surface was investigated before in our group [18,19]. The corresponding results have allowed designing the most stable arrangements for clusters as well as for supramolecular networks at PBE-D2 level of calculation. Table S2 summarizes the stabilization energies and the geometrical parameters. According to these previous results, the most stable geometries of monomer, dimer and 2D-networks presented on Fig. S2 are adsorbed on top of graphene and the complexes are fully optimized.

The monomer is placed on different sites in the (8×8) graphene supercell, and for each adsorption site, the system is fully relaxed. In all cases, at the PBE level, the adsorption reaction of the monomer is endothermic, in contrast with the case of the melamine molecule. When including the dispersion correction, an exothermic adsorption is calculated with a minimum energy of −1.191 eV. The interaction of the NTCDI monomer with graphene induces a very small deformation of graphene (~0.30 Å). The entire NTCDI molecule is flat at an equilibrium distance of about 3.20 Å.

The most stable dimer identified for NTCDI in absence of the surface (See Fig. S2 and Table 2) and on Au(111) surface [17,19] is considered for the adsorption on graphene (11×11) surface and the obtained complexes are fully relaxed. The calculated adsorption energies, at PBE-D2 level were found to be equal to −1.745 eV per molecule, with a large part of dispersion correction, namely −1.210 eV per molecule (See Table 2).

2D-networks containing two molecules per unit cell were identified as stable in vacuum. The most stable is adsorbed on graphene surface. A supercell (4×2) of graphene that commensurates with the molecular network is chosen to describe the adsorption. While the missing fit along an axis is close to 0.1%, it reaches up to 5% along the b axis. The calculated adsorption energy is found to be equal to −0.790 and −1.901 eV per molecule (Table 2) at standard PBE and PBE-D2 levels, respectively. In contrast to melamine, no significant deformation of graphene is observed for the network as well as for the cluster. In the assembly case, all NTCDI molecules are present on the same plane, as well as hydrogen at an equilibrium distance of 3.50 Å (Fig. 4).

According to Table 2, the adsorption energy increases from the monomer to the supramolecular formation, in contrast to what we observed for melamine. The stabilization energy in vacuum (ΔE^{V}_{stab}) decreases from monomer to network (Table S2). Hence, the total stabilization energy decreases importantly with respect to the assembly size. The adsorption is more favorable when the cluster or networks are previously formed. The adsorption of a single molecule is therefore unfavorable. Unlike the case of melamine, these results indicate that the prior formation of the supramolecular network allows its adsorption on graphene.

The association of melamine and NTCDI has been previously investigated because of the resulting porous network which allows to receive a guest molecule inside the pores and to form a complex, for which, one can easily tune the properties through an appropriate selection of invited system [17,18,59]. In the gas phase, the interaction is characterized by the establishment of three hydrogen bonds, corresponding to an interaction energy of −0.944 eV (See Table S3), in agreement with these previous theoretical works [17,18,59].

We now consider the mixed melamine-NTCDI complexes self-assembling properties on graphene. The mixed dimer (NTCDI + melamine) has been placed initially in 3 different positions presented in Fig. 5. The calculated adsorption energies

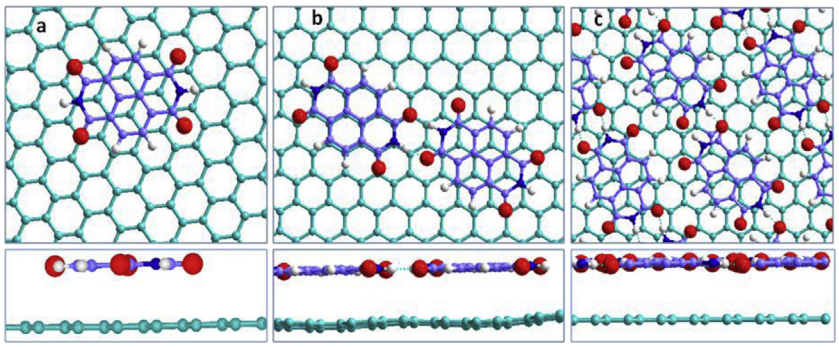

Fig. 4. The different most stable structures of NTCDI monomer (a), dimer (b) and 2D-network (c) on graphene surface.

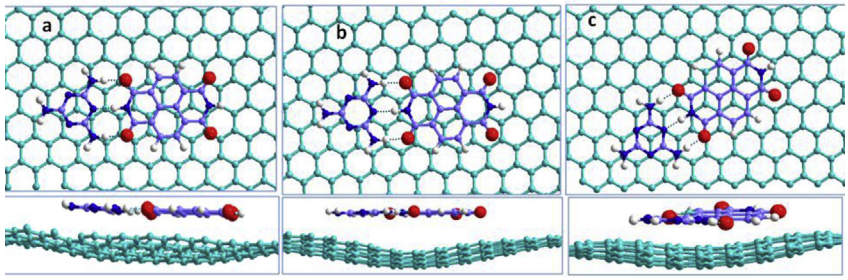

Fig. 5. The different optimized structures of Melamine-NTCDI dimer on a graphene sheet. Configurations A (a), B (b), and C (c).

lie in the range −3.450, −3.582 eV for the three sites (Table 2). In each case, a strong deformation of graphene is observed, in particular under melamine molecule with a buckling height ranging between 1.96 and 2.61 Å.

The contribution of vdW interactions varies from 20 to more than 50% depending on the site. The largest obtained value is due to the increased density of molecules on the surface. The geometry of the two dimensional honeycomb hexagonal network with unit cell containing two melamine and three NTCDI molecules, is built and optimized in vacuum. The stabilization energy (ΔE^{V}_{stab}) reported in Table S3 is found to −5.285 eV corresponding to an average energy by hydrogen bond (ΔE_{LH}) of −0.294 eV. The results are closed to the previous studies [17,18,59]. The unit cell is deposited on a (11 × 11) graphene super cell. The mismatch between the molecular network and graphene surface lattice parameters is less than 3.1%. The adsorption energy is found to be equal to −3.125 eV at the PBE level and is doubled when the dispersion correction is taken into account. The network induces the most important deformation of graphene. Indeed, in the network pores, graphene presents a hill, while under the adsorbed molecules; it forms a valley as shown in Fig. 6. The deformation presents a height between the bottom of the valley and the top of the hill which is measured to be equal to 2.60 Å.

3.3. Graphene deformation analysis

Depending on the density and the nature of assembled molecules, a significant deformation is observed. To analyze this deformation, we define deformation energy as the difference between planar graphene and the buckling. We evaluate the graphene deformation energy ΔE_{def} as the difference between interaction and adsorption energy.

$$\Delta E_{def} = \Delta E_{ads} - \Delta E_{\text{int}}$$

The interaction energy is defined as the difference between the energy of the complex and the energy of the isolated system kept in their complex geometry.

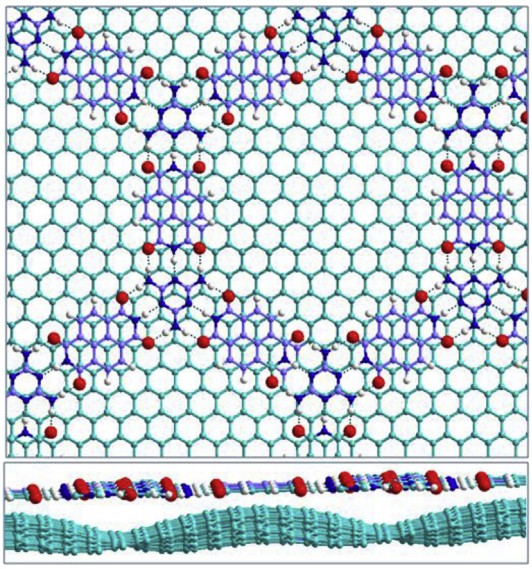

Fig. 6. Top view (top) and side view (bottom) of the Melamine-NTCDI 2D network.

$$\Delta E_{\text{int}} = \frac{\left[E(M_{n,ads}) - nE(M_a) - E(G_a)\right]}{n}$$

As define previously, the adsorption energy is the difference between the energy of the fully relaxed complex and the energies of isolated adsorbate and surface, both relaxed separately.

Table 3 contains the obtained results indicating that the height of the deformation is proportional to the deformation energy. For NTCDI molecules, calculations are performed for a (8 × 8) supercell with a total surface of 368.7 Å^2. We find a slight deformation of 0.36 Å, corresponding to deformation energy close to 0.3 meV per graphene unit cell. In the case of melamine, the maximum deformation is found for the C-top configuration with a buckling height of 1.69 Å corresponding to deformation energy of 0.92 eV (14.4 meV per unit cell). The most important deformation is found for the complex melamine-NTCDI network with a deep height of 2.59 Å, yielding deformation energy of 36.4 meV per unit cell. These deformation energies are weak with respect to the thermic agitation at room temperature. To evaluate the kinetic of deformation in absence of adsorbate, we calculate the barrier of deformation between planar and strongly deformed (Fig. S4). We observe a linear decrease of energy, leading to an absence of energy barrier between the two states. In this case, the buckling of the sheet is a cooperative effect of carbon atoms that keep their sp^2 hybridization. The deformation energy is much smaller than the one obtained for a vertical displacement of one carbon atom that implies several eV [60]. In the later case, the π and σ bonds of the displaced atom are strongly weakened.

Previous studies remain limited [31,53] to the (6 × 6) super cell, probably for computational time reasons. In our study, when the melamine is adsorbed on this super cell, we observed no significant deformation (See Fig. 2). Same result is obtained for the two dimensional networks. In our study, when the single melamine molecule is adsorbed on this unit cell, we observed significant deformation. But in the case of self-assembled molecules, no deformation is observed because of the intermolecular interaction that decouples the network and the surface. We then suppose that the ratio between the adsorbate and the surface super cell, and the density of nitrogen atoms in molecules, are key parameters that induce the buckling of the graphene surface.

According to the theorem of Mermin and Wagner [61], pristine graphene at long range is not planar. It presents an ondulation with a distance between the neighboring hills of about 4 nm. DNA nucleobases adsorption on nanographene show significant curvature due to the possibility of weak hydrogen bond-like interactions involving pyramidal amino groups of the nucleobases and π-center of the nanographene. In their recent studies, Ross and co-authors [62] show that the deposition on metallic surface can reduce the original wavelength and increase the amplitude depending on the rugosity. They use scanning tunneling microscopy to highlight that graphene monolayer supported by a Ru(0001) single crystal reveals a buckling with a periodicity of 30 Å and a height of 1.56 Å. More recently, significant deformation leading to hill and valley formation was observed following the same trend when 2,4 bis (terpyridine) molecules were adsorbed on a graphene sheet. In that case, the periodicity seems to be reduced to 20 Å, which corresponds to the molecule size [63]. In the case of melamine, the diameter is about 6.50 Å, considerably smaller than the buckling periodicity of pristine graphene. Nevertheless, a corrugation with similar height is observed, which shows that the adsorbate influences the buckling periodicity. The ability of suspended graphene sheet to buckle under STM tip with an important deformation achieving the nanometer scale was observed recently through a combination of tunneling effect spectroscopy measurements and molecular dynamic simulations [64]. More recently, graphene deformation under carbon nanocluster is observed [65] In this study, the elastic scattering theory was used to experimentally estimate the rotational energy barriers of molecules on graphene which is found to be within the range of 1.5–12 meV per atom.

3.4. Effect of adsorption on graphene electronic properties

To analyze the nature of the interaction between the melamine and the surface and a possible charge transfer, we have performed the difference of charge densities between the complex and the isolated melamine, and the bare surface $\Delta\rho(r) = \rho_{G\text{-}M}(r) - \rho_G(r) - \rho_M(r)$. A positive value of $\Delta\rho(r)$ allows to locate the electron gain in the complex, whereas a negative value indicates the region of electron depletion.

Fig. 7 shows the regions of electronic gain or depletion for melamine, NTCDI and the complex in interaction with graphene surface. The results show that the type of interaction is different for melamine and NTCDI. While melamine seems to give electron to the surface, the NTCDI attracts electrons from the surface. The maximum value of $\Delta\rho(r)$ is more important for the NTCDI than melamine For the complex, the electron transfer is slightly higher than for the isolated NTCDI, and involves

Table 3
Calculated adsorption and deformation energies of graphene sheet after adsorption and the maximum deformation of the sheet.

System	ΔE_{ads} (eV)	ΔE_{int} (eV)	ΔE_{def} (eV)	ΔE_{def}/unit cell (meV)	Maximum deformation (Å)
Melamine	−1.388	−0.468	0.920	14.38	1.69
NTCDI	−1.191	−1.171	0.020	0.31	0.38
Melamine-NTCDI	−6.895	−2.495	4.400	36.36	2.59

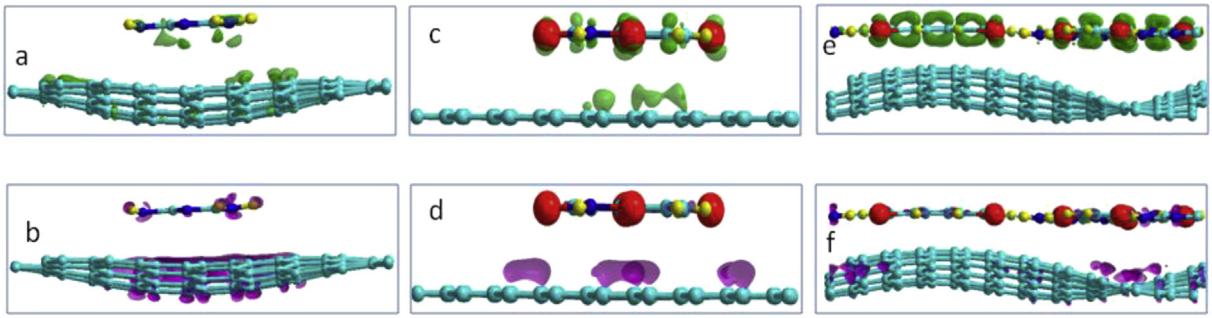

Fig. 7. Difference of charge densities: electron gain ($\Delta\rho(r) > 0$) for melamine (a), NTCDI (b) and the complex melamine-NTCDI (c); electron depletion ($\Delta\rho(r) < 0$) for melamine (d), NTCDI (e) and the complex (f). Note that the maximum values of $\Delta\rho_{max}(r)$ are different for the three systems.

essentially NTCDI molecule and graphene. The strong interaction of NTCDI with melamine seems to promote the acceptor character of NTCDI as well as a stronger charge transfer.

The analysis of electronic densities is in agreement with the deformation which is more pronounced in the case of the complex than for the isolated system. The electron transfer allows to modify the band structure near Fermi level as it can be seen in the density of states of the three systems (Fig. 8).

These observations are in line with the energy levels modifications around Fermi level as shown on Fig. 8. This figure presents the density of states spectra for isolated system adsorbed system on surface. The total DOS of NTCDI on graphene shows that the Fermi level shifted toward lower energies. In the case of melamine, the shift of Fermi level is less important.

By analyzing the projection of the density of states on atomic orbitals (PDOS), we can observe that for melamine, the highest occupied molecular orbital (HOMO) is closer to Fermi level than the lowest unoccupied orbital (LUMO) (Fig. 8). The opposite trend is observed for NTCDI molecule where charge transfer from graphene to molecule is observed, as indicated in the DOS by the shift of the LUMO toward Fermi level (Fig. 8).

We present the band structure of isolated graphene, melamine C-top position on graphene, on Fig. 9. For pristine graphene, the linear dispersion of valence and conduction bands in the high symmetry K point can be observed. In the case of the adsorption of a monomer C-top, the gap opens slightly, and reaches a value close to 87 meV. This gap opening reflects the deformation of graphene below melamine molecule. In the case of NTCDI, a band gap of 100 meV is found. This value is closed to the previous experimental value found for the PTCDI molecule (~80 meV) [66]. These results are in line with the bands behavior near Fermi level observed in the total DOS presented before in Fig. 8. In contrast with the porous hexagonal lattice of melamine, the gap is lower with a value smaller than 10 meV, in line with the weak interaction between the molecular networks. These results remain however still qualitative and depend strongly on the calculation method and the size of the cells. However, they remain within the range of values found in the literature for similar systems. The band gap opening of graphene under planar molecule was observed before for triazine and borazine with values of 62.9 and 45 meV respectively [53]. Exploring the role of defects and doping in graphene, Terrones et al. found a band gap opening in the cases of doping by silicon, boron and nitrogen [67]. A small band gap of 24 meV was observed for single melamine adsorbed on a pristine (6×6) graphene, while more important band gap of 90 meV, was observed for defective graphene [32].

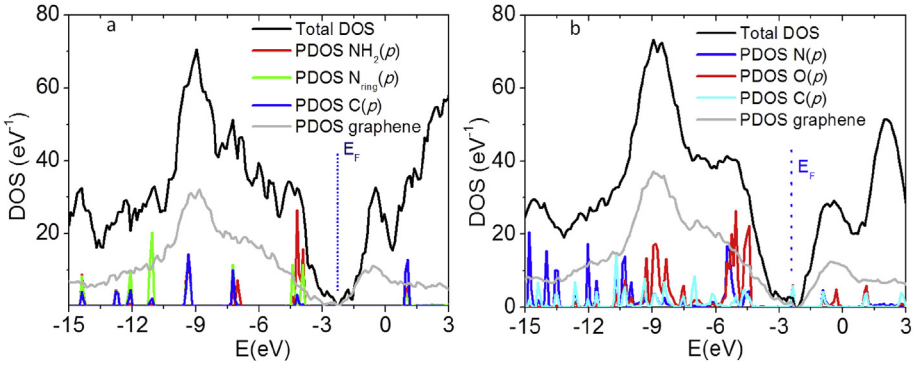

Fig. 8. Total DOS (black) of melamine/graphene in the C-top configuration (a) and PDOS on 2*p* orbitals of Nsp^3 (red), Nsp^2 (green) and C (blue) for melamine. Total DOS of NTCDI/graphene (b) and the PDOS on 2*p* orbital sod N(blue), O(red) and C(cyan) for NTCDI. (For interpretation of the references to colour in this figure legend, the reader is referred to the web version of this article.)

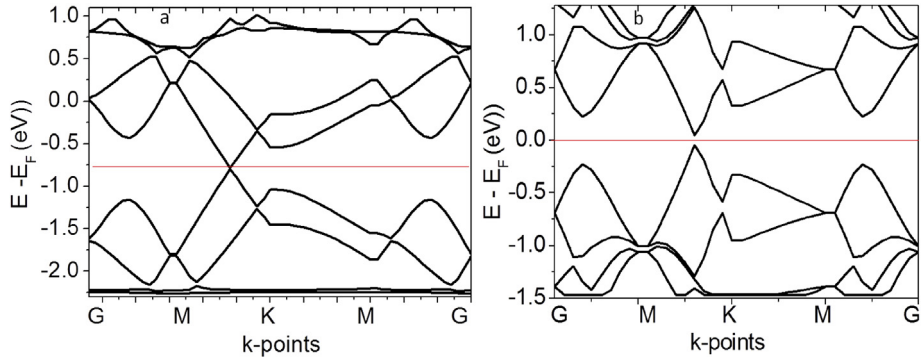

Fig. 9. Band structure of a) pristine graphene and b) graphene under melamine adsorption in C_top configuration.

4. Conclusion

In this paper, we have used first-principles simulations to study the assembly of functional molecules on graphene. We have optimized the geometries of our aggregates and networks in the presence and absence of the surfaces and we have calculated their stabilization and adsorption energies. The electronic properties of the most stable systems are computed and allow to interpret adsorption effects on graphene.

The results show that in the absence of surface, the most stable melamine networks are hexagonal compact lattices in absence of surface and switch to the hexagonal porous structure when a planar symmetry is imposed. In both cases, stability is provided by two hydrogen bonds between neighboring molecules. The complex melanine/NTCDI is formed by three hydrogen bonds between adjacent molecules which makes it particularly stable. The contribution of vdW forces is necessary to describe the energetic aspects of the assembly as well as the adsorption processes.

The adsorption process is different for melamine and NTCDI. While the adsorption energy increases with the size of assembly for melamine, it decreases for NTCDI. The contribution of vdW forces is even more important. For low coverage rate, depending on the supercell size and the density of nitrogen atoms in the molecular complex (two molecules on a (8×8) super cell), the supporting graphene network is significantly distorted. This deformation occurs mainly under the nitrogen atoms and generates a buckling in the graphene sheet with a corrugation achieving 2.59 Å. The study of electronic properties reveals a different type of electron transfer for melamine and NTCDI. While for melamine a charge transfer from the molecule toward the surface is observed, we obtain an opposite result for NTCDI. In both cases, the effect of adsorption process on graphene shows a gap opening at low coverage rate.

Acknowledgements

This work was performed using HPC resources from GENCI- [CCRT/CINES/IDRIS] (Grant 2016-[c2016097006]). We acknowledge the financial support from the French Government's Investissementsd'Avenir program: Laboratoired'Excellence ‘Sciences and Engineering for Advanced Materials and devices – SEAMs’ (grant no. ANR-10-LABX-96).

Appendix A. Supplementary data

Supplementary data related to this article can be found at http://dx.doi.org/10.1016/j.spmi.2017.03.034.

References

[1] V. Georgakilas, M. Otyepka, A.B. Bourlinos, V. Chandra, N. Kim, K.C. Kemp, P. Hobza, R. Zboril, K.S. Kim, Functionalization of graphene: covalent and non-covalent approaches, derivatives and applications, Chem. Rev. 112 (2012) 6156–6214.
[2] M.C. Daniel, D. Astruc, Gold nanoparticles: assembly, supramolecular chemistry, quantum-size-related properties, and applications toward biology, catalysis, and nanotechnology, Chem. Rev. 104 (2004) 293–346.
[3] M.O. Lorenzo, C.J. Baddeley, C. Muryn, R. Raval, Extended surface chirality from supramolecular assemblies of adsorbed chiral molecules, Nature 404 (2000) 376–379.
[4] E. Busseron, Y. Ruff, E. Moulin, N. Giuseppone, Supramolecular self-assemblies as functional nanomaterials, Nanoscale 5 (2013) 7098–7140.
[5] C. Fu, H.-P. Lin, J.M. Macleod, A. Krayev, F. Rosei, D.F. Perepichka, Unravelling the self-assembly of hydrogen bonded NDI semiconductors in 2D and 3D, Chem. Mater. 28 (2016) 951–961.
[6] X. Lefèvre, F. Moggia, O. Segut, Y.-P. Lin, Y. Ksari, G. Delafosse, K. Smaali, D. Guérin, V. Derycke, D. Vuillaume, S. Lenfant, L. Patrone, B. Jousselme, Influence of molecular organization on the electrical characteristics of π-conjugated self-assembled monolayers, J. Phys. Chem. C 119 (2015) 5703–5713.
[7] Y. Zang, T. Aoki, M. Teraguchi, T. Kaneko, L. Ma, H. Jia, Two-dimensional and related polymers: concepts, synthesis, and their potential application as separation membrane materials, Polym. Rev. 55 (2015) 57–89.
[8] H. Chang, H. Wu, Graphene-based nanocomposites: preparation, functionalization, and energy and environmental applications, Energy Environ. Sci. 6 (2013) 3483–3507.

[9] L. Voorhaar, R. Hoogenboom, Supramolecular polymer networks: hydrogels and bulk materials, Chem. Soc. Rev. 45 (2016) 4013–4031.
[10] P. Lang, Z. Qin, V. Noel, M. Seydou, N. Battaglini, S. Zrig, G. Anquetin, F. Maurel, B. Piro, M.C. Pham, Nanodomains of juglonethiol on Au(111): relationship between domain size and electrochemical properties, J. Phys. Chem. C 119 (2015) 29015–29026.
[11] R.E.A. Kelly, W. Xu, M. Lukas, R. Otero, M. Mura, Y.J. Lee, E. Laegsgaard, I. Stensgaard, L.N. Kantorovich, F. Besenbacher, An investigation into the interactions between self-assembled adenine molecules and a Au(111) surface, Small 4 (2008) 1494–1500.
[12] M. Mura, A. Gulans, T. Thonhauser, L. Kantorovich, Role of van der Waals interaction in forming molecule-metal junctions: flat organic molecules on the Au(111) surface, Phys. Chem. Chem. Phys. 12 (2010) 4759–4767.
[13] M. Mura, N. Martsinovich, L. Kantorovich, Theoretical study of melamine superstructures and theirs interaction with Au(111) surface, Nanotechnology 19 (2008) 465704.
[14] M. Mura, F. Silly, G.A.D. Briggs, M.R. Castell, L.N. Kantorovich, H-bonding supramolecular assemblies of PTCDI molecules on the Au(111) surface, J. Phys. Chem. C 113 (2009) 21840–21848.
[15] M. Mura, X. Sun, F. Silly, H.T. Jonkman, G.A.D. Briggs, M.R. Castell, L.N. Kantorovich, Experimental and theoretical analysis of H-bonded supramolecular assemblies of PTCDA molecules, Phys. Rev. B 81 (2010).
[16] M. Sassi, V. Oison, J.M. Debierre, First principle study of a bimolecular thin film on Ag(111) surface, Surf. Sci. 602 (2008) 2856–2862.
[17] A. Ciesielski, C.-A. Palma, M. Bonini, P. Samorì, Towards supramolecular engineering of functional nanomaterials: pre-programming multi-component 2D self-assembly at solid-liquid interfaces, Adv. Mater. 22 (2010) 3506–3520.
[18] J. Teyssandier, N. Battaglini, M. Seydou, G. Anquetin, B. Diawara, X. Sun, F. Maurel, P. Lang, Elaboration of hydrogen-bonded 2D supramolecular assemblies on Au(111) from solutions: toward naphthalene tetracarboxylic diimide-melamine nanoporous networks, J. Phys. Chem. C 117 (2013) 8737–8745.
[19] M. Seydou, J. Teyssandier, N. Battaglini, G.T. Kenfack, P. Lang, F. Tielens, F. Maurela, B. Diawara, Characterization of NTCDI supra-molecular networks on Au(111); combining STM, IR and DFT calculations, RSC Adv. 4 (2014) 25698.
[20] S.P. Jarvis, A.M. Sweetman, I. Lekkas, N.R. Champness, L. Kantorovich, P. Moriarty, Simulated structure and imaging of NTCDI on Si(1 1 1)-7 $\times$ 7 : a combined STM, NC-AFM and DFT study, J. Phys. Condens. Matter 27 (2015) 054004.
[21] X. Zhang, T. Chen, Q. Chen, L. Wang, L.-J. Wan, Self-assembly and aggregation of melamine and melamine-uric/cyanuric acid investigated by STM and AFM on solid surfaces, Phys. Chem. Chem. Phys. 11 (2009) 7708–7712.
[22] S.K.M. Henze, O. Bauer, T.L. Lee, M. Sokolowski, F.S. Tautz, Vertical bonding distances of PTCDA on Au(111) and Ag(111): relation to the bonding type, Surf. Sci. 601 (2007) 1566–1573.
[23] E. Rauls, S. Blankenburg, W.G. Schmidt, Chemical reactivity on surfaces: modeling the imide synthesis from DATP and PTCDA on Au(111), Phys. Rev. B 81 (2010).
[24] X.N. Sun, M. Mura, H.T. Jonkman, L.N. Kantorovich, F. Silly, Fabrication of a complex two-dimensional adenine-perylene-3,4,9, 10-tetracarboxylic dianhydride chiral nanoarchitecture through molecular self-assembly, J. Phys. Chem. C 116 (2012) 2493–2499.
[25] K.S. Novoselov, A.K. Geim, S.V. Morozov, D. Jiang, Y. Zhang, S.V. Dubonos, I.V. Grigorieva, A.A. Firsov, Electric field effect in atomically thin carbon films, Science 306 (2004) 666–669.
[26] D. Chen, L. Tang, J. Li, Graphene-based materials in electrochemistry, Chem. Soc. Rev. 39 (2010) 3157–3180.
[27] Z. Liu, S.P. Lau, F. Yan, Functionalized graphene and other two-dimensional materials for photovoltaic devices: device design and processing, Chem. Soc. Rev. 44 (2015) 5638–5679.
[28] P. Miro, M. Audiffred, T. Heine, An atlas of two-dimensional materials, Chem. Soc. Rev. 43 (2014) 6537–6554.
[29] X. Zhuang, Y. Mai, D. Wu, F. Zhang, X. Feng, Two-dimensional soft nanomaterials: a fascinating world of materials, Adv. Mater. 27 (2015) 403–427.
[30] M. Seydou, S. Marsaudon, J. Buchoux, J.P. Aimé, A.M. Bonnot, Molecular mechanics investigations of carbon nanotube and graphene sheet interaction, Phys. Rev. B 80 (2009) 245421.
[31] X. Zhang, T. Chen, Q. Chen, L. Wang, L.-J. Wan, Self-assembly and aggregation of melamine and melamine-uric/cyanuric acid investigated by STM and AFM on solid surfaces, Phys. Chem. Chem. Phys. 11 (2009) 7708–7712.
[32] H. Medina, Y.-C. Lin, D. Obergfell, P.-W. Chiu, Tuning of charge densities in graphene by molecule doping, Adv. Funct. Mater. 21 (2011) 2687–2692.
[33] Z. Zhang, H. Huang, X. Yang, L. Zang, Tailoring electronic properties of graphene by π-π stacking with aromatic molecules, J. Phys. Chem. Lett. 2 (2011) 2897–2905.
[34] H. Yang, A.J. Mayne, G. Comtet, G. Dujardin, Y. Kuk, P. Sonnet, L. Stauffer, S. Nagarajane, A. Gourdone, STM imaging, spectroscopy and manipulation of a self-assembled PTCDI monolayer on epitaxial graphene, Phys. Chem. Chem. Phys. 15 (2013) 4939.
[35] S. Vojtech, H. Pavel, R. Jan, Free-energy simulations of hydrogen bonding versus stacking of nucleobases on a graphene surface, J. Phys. Chem. C 115 (2011) 19455–19462.
[36] P.I. Järvinen, S.K. Hämäläinen, M. Ijäs, Ari Harju, P. Liljeroth, Self-assembly and orbital imaging of metal phthalocyanines on a graphene model surface, J. Phys. Chem. C 118 (2014) 13320–13325.
[37] S.J. Altenburg, M. Lattelais, B. Wang, M.-L. Bocquet, R. Berndt, Reaction of phthalocyanines with graphene on Ir(111), J. Am. Chem. Soc. 137 (2015) 9452–9458.
[38] R.N. Gunasinghe, D.G. Reuven, K. Suggs, X.-Q. Wang, Filled and empty orbital interactions in a planar covalent organic framework on graphene, J. Phys. Chem. Lett. 3 (2012) 3048–3052.
[39] X. Zeng, S. Chang, K. Deng, J. Zhang, H. Sun, Q. Zeng, J. Xie, Synthesis and molecular structures of BINOL complexes: an STM investigation of 2D self-assembly, Cryst. Growth Des. 15 (2015) 3096–3100.
[40] J.M. MacLeod, J.A. Lipton-Duffin, D. Cui, S.D. Feyter, F. Rosei, Substrate effects in the supramolecular assembly of 1,3,5-benzene tricarboxylic acid on graphite and graphene, Langmuir 31 (2015) 7016–7024.
[41] B. Wanno, C. Tabtimsai, A DFT investigation of CO adsorption on VIIIB transition metal-doped graphene sheets, Superlattices Microstruct. 67 (2014) 110–117.
[42] S. Rahali, Y. Belhocine, J. Touzeau, B. Tangour, F. Maurel, M. Seydou, Balance between physical and chemical interactions of second-row diatomic molecules with graphene sheet, Superlattices Microstruct. 102 (2017) 45–55.
[43] A.H. Mashhadzadeh, A.M. Vahedi, M. Ardjmand, M.G. Ahangari, Investigation of heavy metal atoms adsorption onto graphene and graphdiyne surface: a density functional theory study, Superlattices Microstruct. 100 (2016) 1094–1102.
[44] S. Grimme, Density functional theory with London dispersion corrections, Wiley Interdiscip. Rev. Comput. Mol. Sci. 1 (2011) 211–228.
[45] G. Kresse, J. Hafner, Ab-initio molecular-dynamics for liquid-metals, Phys. Rev. B 47 (1993) 558–561.
[46] G. Kresse, J. Hafner, Ab-initio molecular-dynamics simulation of the liquid-metal amorphous-semiconductor transition in germanium, Phys. Rev. B 49 (1994) 14251–14269.
[47] P.E. Blochl, Projector augmented-wave method, Phys. Rev. B 50 (1994) 17953–17979.
[48] G. Kresse, D. Joubert, From ultrasoft pseudopotentials to the projector augmented-wave method, Phys. Rev. B 59 (1999) 1758–1775.
[49] B. Hammer, L.B. Hansen, J.K. Norskov, Improved adsorption energetics within density-functional theory using revised Perdew-Burke-Ernzerhof functionals, Phys. Rev. B 59 (1999) 7413–7421.
[50] J.P. Perdew, K. Burke, M. Ernzerhof, Generalized gradient approximation made simple (vol 77, pg 3865, 1996), Phys. Rev. Lett. 78 (1997), 1396–1396.
[51] S. Grimme, Semiempirical GGA-type density functional constructed with a long-range dispersion correction, J. Comput. Chem. 27 (2006) 1787–1799.
[52] V. León, A.M. Rodriguez, P. Prieto, M. Prato, E. Vázquez, Exfoliation of graphite with triazine derivatives under ball-milling conditions: preparation of few-layer graphene via selective noncovalent interactions, ACS Nano 8 (2014) 563–571.
[53] C.-H. Chang, X. Fan, L.-J. Li, J.-L. Kuo, Band gap tuning of graphene by adsorption of aromatic molecules, J. Phys. Chem. C 116 (2012) 13788–13794.

[54] E.G. Gordeev, M.V. Polynski, V.P. Ananikov, Fast and accurate computational modeling of adsorption on graphene: a dispersion interaction challenge, Phys. Chem. Chem. Phys. 15 (2013) 18815–18821.
[55] M. Seydou, Y.J. Dappe, S. Marsaudon, J.P. Aimé, X. Bouju, A.M. Bonnot, Atomic force microscope measurements and LCAO-S2 + vdW calculations of contact length between a carbon nanotube and a graphene, Surf. Phys. Rev. B 83 (2011) 045410.
[56] P.A. Denis, Chemical reactivity of electron-doped and hole-doped graphene, J. Phys. Chem. C 117 (2013) 3895–3902.
[57] S. Panigrahi, A. Bhattacharya, S. Banerjee, D. Bhattacharyya, Interaction of nucleobases with wrinkled graphene surface: dispersion corrected DFT and AFM studies, J. Phys. Chem. C 116 (2012) 4374–4379.
[58] W. Song, N. Martsinovich, W.M. Heckl, M. Lackinger, Born–Haber cycle for monolayer self-assembly at the liquid–solid interface: assessing the enthalpic driving force, J. Am. Chem. Soc. 135 (2013) 14854–14862.
[59] J. Wen, J. Ma, Modulating morphology of thiol-based monolayers in honeycomb hydrogen-bonded nanoporous templates on the Au(111) surface: simulations with the modified force field, J. Phys. Chem. C 116 (2012) 8523–8534.
[60] M. Pizzochero, M. Bonfanti, R. Martinazzo, Hydrogen on silicone: like or unlike graphene? Phys. Chem. Chem. Phys. 18 (2016) 15654–15666.
[61] N.D. Mermin, H. Wagner, Absence of ferromagnetism or antiferromagnetism in one- or two dimensional isotropic, Phys. Rev. Lett. 17 (1966) 1133–1136.
[62] M. Roos, D. Künzel, B. Uhl, H.-H. Huang, O.B. Alves, H.E. Hoster, A. Gross, R.J.u. Behm, Hierarchical interactions and their influence upon the adsorption of organic molecules on a graphene film, J. Am. Chem. Soc. 133 (2011) 9208–9211.
[63] M. Mura, F. Silly, Experimental and theoretical analysis of hydrogen bonding in two-dimensional chiral 4′,4‴-(1,4-Phenylene)bis(2,2′:6′,2″-terpyridine) self-assembled nanoarchitecture, J. Phys. Chem. C 119 (2015) 27125–27130.
[64] R. Breitwieser, Y.-C. Hu, Y.C. Chao, R.-J. Li, Y.R. Tzeng, L.-J. Li, S.-C. Liou, K.C. Lin, C.W. Chen, W.W. Pai, Flipping nanoscale ripples of free-standing graphene using a scanning tunneling microscope tip, Carbon 77 (2014) 236–243.
[65] J. Choe, Y. Lee, L. Fang, G.-D. Lee, Z. Bao, K. Kim, Direct imaging of rotating molecules anchored on graphene, Nanoscale 8 (2016) 13174–13180.
[66] S.M. Kozlov, F. Viñes, A. Görling, Bandgap engineering of graphene by physisorbed adsorbates, Adv. Mater. 23 (2011) 2638–2643.
[67] H. Terrones, R. Lv, M. Terrones, M.S. Dresselhaus, The role of defects and doping in 2D graphene sheets and 1D nanoribbons, Rep. Programme. Phys. 75 (2012) 062501.